The EMBO Journal Vol.17 No.11 pp.3005–3015, 1998

HIF-1α is required for solid tumor formation and embryonic vascularization

Heather E.Ryan, Jessica Lo and Randall S.Johnson[1,2,3]

Department of Biology, [1]Center for Molecular Genetics and [2]UCSD Cancer Center, University of California, San Diego, La Jolla, CA 92093-0366, USA

[3]Corresponding author
e-mail: rjohnson@biomail.ucsd.edu

The transcriptional response to lowered oxygen levels is mediated by the hypoxia-inducible transcription factor (HIF-1), a heterodimer consisting of the constitutively expressed aryl hydrocarbon receptor nuclear translocator (ARNT) and the hypoxic response factor HIF-1α. To study the role of the transcriptional hypoxic response *in vivo* we have targeted the murine HIF-1α gene. Loss of HIF-1α in embryonic stem (ES) cells dramatically retards solid tumor growth; this is correlated with a reduced capacity to release the angiogenic factor vascular endothelial growth factor (VEGF) during hypoxia. HIF-1α null mutant embryos exhibit clear morphological differences by embryonic day (E) 8.0, and by E8.5 there is a complete lack of cephalic vascularization, a reduction in the number of somites, abnormal neural fold formation and a greatly increased degree of hypoxia (measured by the nitroimidazole EF5). These data demonstrate the essential role of HIF-1α in controlling both embryonic and tumorigenic responses to variations in microenvironmental oxygenation.

Keywords: gene targeting/HIF-1α/hypoxia/tumorigenesis

Introduction

Hypoxia causes a wide range of responses in an organism at both the systemic and cellular levels (Bunn and Poyton, 1996). Lowered environmental oxygen levels cause increased erythropoietin (EPO) production, which results in higher oxygen-carrying capacity in the blood (Blanchard *et al*., 1993). Decreased oxygen pressure in interstitial fluid results in a metabolic switch to glycolysis for energy production (Semenza *et al*., 1994). In addition, hypoxia causes secretion of vascular endothelial growth factor (VEGF) (Shweiki *et al*., 1992; Ladoux and Frelin, 1993; Banai *et al*., 1994; Ikeda *et al*., 1995; Levy *et al*., 1995; Liu *et al*., 1995; Pe'er *et al*., 1995; Shima *et al*., 1995; Stone *et al*., 1995), an angiogenic/permeability factor which acts to increase the immediate availability of oxygen from capillaries (through increased vascular permeability) as well as induce formation of new vessels.

The hypoxic induction of angiogenesis is a hallmark of pathological processes such as wound healing and solid tumor formation; it is strongly correlated with the disrupted circulation and rapid growth characteristic of those states. In addition, hypoxic regions within tumors are resistant to radiotherapy and thus constitute an extremely important fraction of cancer cells from a clinical perspective (Brown and Giaccia, 1994; Dachs *et al*., 1997). These hypoxic areas of the tumor form a depot of cells resistant to p53-mediated apoptosis and are thus likely locations of selection for mutations in p53 prior to invasive growth and metastasis (Graeber *et al*., 1996).

One component of the hypoxic response is transcriptional activation, which is mediated by binding of the hypoxia-inducible transcription factor, HIF-1, to an 8 bp hypoxia response element (HRE), an enhancer found in genes subject to transcriptional regulation by oxygen pressure (Semenza *et al*., 1991; Semenza and Wang, 1992; Wang and Semenza, 1993a,b). The binding moiety of HIF-1 is a heterodimer of the helix–loop–helix (HLH)/PAS proteins HIF-1α and aryl hydrocarbon receptor nuclear translocator (ARNT) (Wang and Semenza, 1995; Wang *et al*., 1995). HIF-1α is the hypoxically responsive component of this complex, while ARNT is expressed constitutively and dimerizes with a number of other HLH proteins, including the PAS proteins Per, Sim, and the aryl hydrocarbon receptor (AhR) (Swanson and Bradfield, 1993; Rowlands and Gustafsson, 1997). A recently cloned homolog of ARNT, ARNT2, has also been shown to participate in heterodimeric DNA binding with AhR and Sim, but its expression is limited to the neural tube (Hirose *et al*., 1996). Targeted null mutations of the ARNT and the AhR genes have widely varying phenotypes in mice. The ARNT mutation causes a mid-gestation retardation of growth first evident at embryonic day (E) 9.5 (Maltepe *et al*., 1997), whereas the AhR knockout mice exhibit a high degree of post-natal mortality and greatly diminished tolerance of xenobiotic compounds (Fernandez-Salguero *et al*., 1995; Schmidt *et al*., 1996).

Due to ARNT's role in processes other than hypoxic induction, we chose to create a null mutation at the HIF-1α locus via homologous recombination in mouse embryonic stem (ES) cells (Papaioannou and Johnson, 1992) in order to investigate the role of the hypoxic response *in vivo*. ES cells lacking HIF-1α are unable to up-regulate several HIF-1 target genes under hypoxic or low glucose conditions, with the most severe effect seen on several enzymes in the glycolytic pathway. Even more striking is the finding that HIF-1α null ES cells form teratocarcinomas one quarter the size of tumors derived from wild-type ES cells. In addition, HIF-1α null embryos display abnormal neural development beginning at E8.0. There is a failure of the neural tube to close, and this failure correlates with the absence of cephalic vascularization, loss of neural tube expression of at least one glycolytic enzyme (phosphoglycerate kinase) and greatly increased neuroectodermal hypoxia and apoptosis.

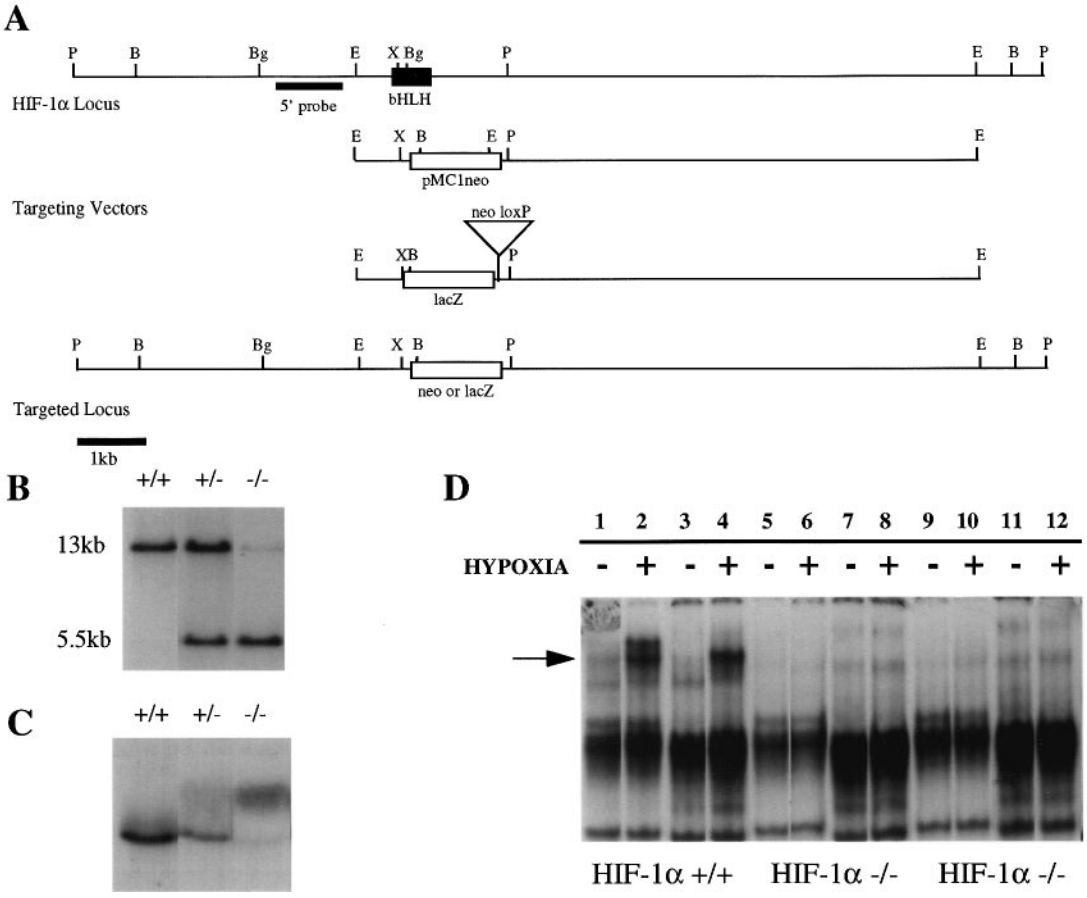

Fig. 1. Targeted disruption of the mouse HIF-1α gene. (**A**) Part of the wild-type HIF-1α locus, the two targeting vectors used and the targeted locus. The HIF-1α gene was disrupted by replacement of the HLH with either a neomycin resistance gene alone (pMC1neo) or an in-frame fusion of the *lacZ* gene followed by a *loxP*-flanked pMC1neo. B, *Bam*HI; Bg, *Bgl*II; E, *Eco*RI; P, *Pst*I; X, *Xba*I. Homologous recombination at the HIF-1α locus introduces a new *Bam*HI site. This results in a 5.5 kb targeted band versus a 13 kb endogenous band upon digestion of genomic DNA with *Bam*HI and hybridization to a 5′ external probe. (**B**) Southern blot analysis of genomic DNA showing correct targeting of the HIF-1α allele. Genomic DNA was isolated from R1 ES cells (Nagy and Rossant, 1992), digested with *Bam*HI and hybridized with the 5′ probe. HIF-1α –/– cells were generated via high G418 selection (Mortensen *et al*., 1992). (**C**) Northern blot analysis of total RNA. Thirty μg of total RNA was loaded per lane and hybridized with a 345 bp HIF-1α cDNA probe. (**D**) Electromobility shift assay on normoxic and hypoxic (1%O_2 for 5 h) nuclear extracts from wild-type and HIF-1α null ES cells. Two binding sites were used: the 18 bp HRE from the EPO gene (Semenza and Wang, 1992) and the 24 bp HRE from the VEGF gene (Forsythe *et al*., 1996). Lanes 1, 2, 5, 6, 9 and 10 contain extracts incubated with the EPO HRE. Lanes 3, 4, 7, 8, 11 and 12 contain extracts incubated with the VEGF HRE. Wild-type ES cells exhibit a shift under hypoxia with either binding site (lanes 2 and 4, arrow). HIF-1α null ES cells do not show a shift under hypoxia with either binding site (lanes 6, 8, 10 and 12).

Results

Generation of HIF-1α-deficient ES cells

The HIF-1α gene was disrupted by two different vectors: one resulting in a null mutation through a replacement of the HLH domain of HIF-1α with a neomycin resistance cassette. The second was a 'knock-in' vector, which produces an in-frame fusion to the *lacZ* gene followed by a *loxP*-flanked neomycin resistance gene (Figure 1A). The neomycin resistance gene in the second targeting vector was removed through the transient transfection of a *cre* expression vector; this was done to prevent interference of the neomycin resistance gene with HIF-1α-driven *lacZ* expression. After successful targeting of the locus with both vectors, HIF-1α null ES cells were generated by high G418 selection (Mortensen *et al*., 1992) and analyzed by Southern and Northern blot analyses (Figure 1B and C). To further confirm that these ES cells contain no functional HIF-1α, we performed electromobility shift assays on wild-type and null cells exposed to hypoxia (Figure 1D). Wild-type ES cells demonstrate a mobility shift under hypoxic conditions while null cells have lost the ability to bind the HRE in a hypoxia-specific manner (Figure 1D). This verifies that functional HIF-1 has been abolished in the HIF-1α null cells.

HIF-1α is essential for up-regulation of a wide range of hypoxically responsive genes

The targeted ES cells allowed us to compare mRNA levels of hypoxia-responsive genes in mutant cell lines with those in wild-type cells under hypoxia (Figure 2A) and glucose deprivation (Figure 2B). In addition, we quantitated the levels of target gene expression in order to determine the exact role of HIF-1α-dependent gene regulation during hypoxia (Figure 2C). The most dramatic effects of the null mutation were seen in glycolytic enzymes, and reveal that HIF-1α is essential for constitutive expression as well as hypoxic induction of phosphoglycerate kinase-1 (PGK) and lactate dehydrogenase A (LDH). Aldolase A (ALDA) is unaffected at the 0 time point and so is not dependent on HIF-1α for basal regulation, but both it and

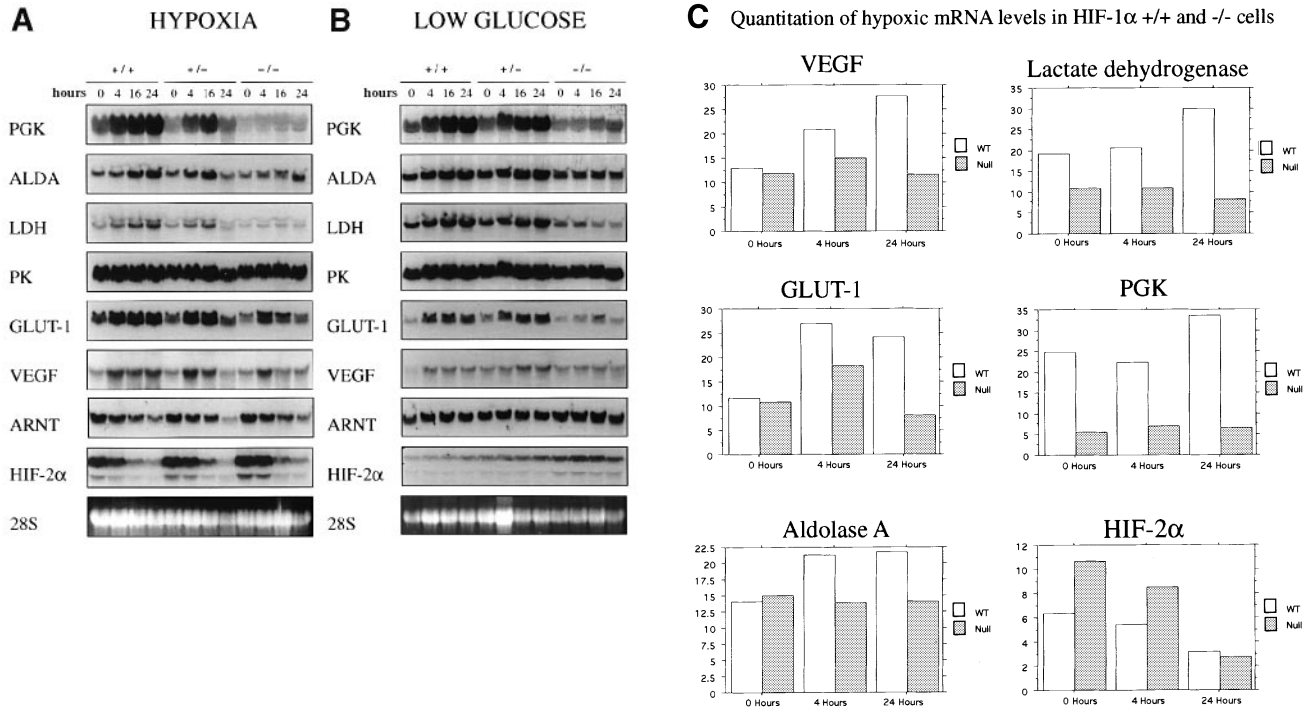

Fig. 2. Northern blot analysis of several HIF-1 target genes from cells cultured under hypoxia (**A**) or low glucose (**B**) conditions. Thirty μg of total RNA was loaded per lane and hybridized to cDNA probes from the following genes: PGK, ALDA, LDH, PK, GLUT1, VEGF, EPO, ARNT and HIF-2α. Equal loading was monitored by ethidium bromide staining of 28S rRNA. (**C**) Phosphorimage analysis of HIF-1 target genes from cells cultured under hypoxic conditions. Ten μg of total RNA was loaded per dot, hybridized to cDNA probes and quantified with a phosphorimager and ImageQuaNT software (both Molecular Dynamics).

the glucose transporter-1 (GLUT1) gene exhibit a greatly reduced capacity for hypoxic and hypoglycemic induction in the null cells.

VEGF is both hypoxically responsive and essential for normal embryonic development (Carmeliet *et al*., 1996; Ferrara *et al*., 1996). Despite complete loss of binding to the VEGF HRE in the HIF-1α null cells (Figure 1D), the hypoxic response of the VEGF gene is only partially eliminated (Figure 2A and C), although quantitation of the signal (Figure 2C) shows that the remaining hypoxic response is marginal and transient. The remaining response is probably due to hypoxically induced stabilization of the VEGF mRNA, which is mediated independently through an element in the 3′-untranslated region (3′ UTR) of the VEGF transcript (Levy *et al*., 1995, 1996; Liu *et al*., 1995; Damert *et al*., 1997). The partial reduction in the hypoxic response of VEGF at the mRNA level was roughly equivalent to that at the protein level at later time points, as assayed by secretion of VEGF from hypoxically induced HIF-1α null cells (Figure 4B), although there is a more severe reduction in the protein level seen at the final point (72 h). This probably reflects accumulation of VEGF in the conditioned medium dictated by the differential rates depicted in the assay for mRNA levels.

HIF-2α is a recently cloned HIF-1α homolog which can also form heterodimers with the ARNT protein (Ema *et al*., 1997; Hogenesch *et al*., 1997; Tian *et al*., 1997). However, no evidence for the presence of HIF-2α–ARNT dimers is seen at the level of DNA binding in HIF-1α null ES cells (Figure 1D). Basal expression of the HIF-2α gene transcript was up almost 50% in HIF-1α null cells (Figure 2C), indicating a possible auto-regulation of the component members of this complex. As a number of other investigators have reported, we saw total transcript levels of HIF-2α, HIF-1α and ARNT decline over time in hypoxic conditions; this has been reported as evidence of increased protein stability as a primary mechansim of HIF-1 induction.

Reduced tumor mass and increased apoptosis in HIF-1α-deficient teratocarcinomas

ES cells have the capacity to form teratocarcinomas when injected into syngeneic or immunocompromised mice. We exploited this property to determine the effect of the HIF-1α null mutation on solid tumor formation.

We found that the null cells are greatly compromised in their ability to form tumors (Figure 4A). Interestingly, the retardation in the formation of the tumors is not evident until later time points; in the first 9 days of tumor growth, the HIF-1α null tumors have approximately the same mass as wild-type tumors (Figure 4A). It is only in the second and third week of tumor growth that differences in size become apparent, finally resulting in a 75% reduction in the size of the null tumors in comparison with the wild-type after 3 weeks. This is correlated with a 40% reduction in tumor vessel density (Figure 4C). This is also demonstrated in the histology shown in Figure 4D, where both vessel density and vessel morphology are clearly altered in the HIF-1α null tumors.

This reduction in tumor volume as tumor mass increases could also conceivably be due to differences in cell growth rates, especially within the hypoxic and typically inefficiently vascularized tumor microenvironment. As can be seen in Figure 3A and B, cell growth rates of the wild-type and null cells in culture are virtually identical in low glucose and hypoxic conditions. This indicates that the

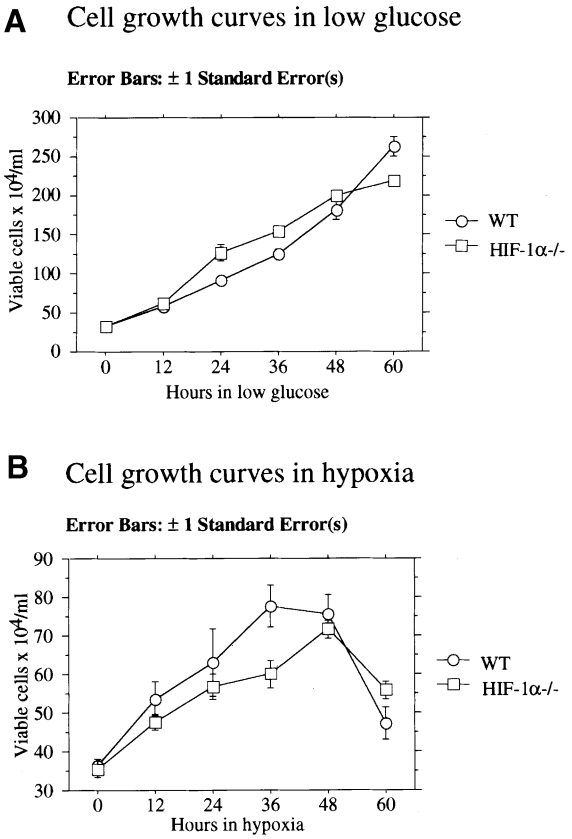

Fig. 3. Cell viability curves under low glucose (**A**) and hypoxia (**B**). Cells were cultured for the indicated times, stained with trypan blue and viable cells were counted.

difference in tumor size is probably due to an alteration in the tumor microenvironment of HIF-1α null tumors, and is not simply a cell autonomous defect.

In order to determine what factors might be causing the reduced tumor volume, we analyzed the tumors for increased hypoxia, as measured by the immunofluorescently detectable marker EF5. Although this marker detected profound differences in the oxygenation of HIF-1α null embryos (see below), there were no reproducible differences in tumor binding of the marker (data not shown). This may be due to the characteristic heterogeneity of individual teratocarcinomas, which are prone to widely varying levels of internal differentiation as they expand.

One factor contibuting to the reduced mass of the null tumors is a clear increase in the amount of apoptosis in the non-necrotic, undifferentiated sections of the tumor. As can be seen in Figure 4E, tumor apoptosis is increased in these non-necrotic regions of nested germ cells. This was difficult to quantify in the teratocarcinomas as a whole, however, due to the large variations in cell density, degree of necrosis and differentiation of the tumors. Further characterization of apoptotic frequency and tumor expansion will require a more uniform tumor type to be derived from HIF-1α null cell lines. One mechanism for this will certainly involve the generation of mice carrying inducible HIF-1α alleles from which differentiated tissue can be derived and transformed, and we currently are pursuing this strategy to define the role of HIF-1 in tumorigenesis more clearly.

Loss of HIF-1α results in disorganized yolk sac vascularization

HIF-1α heterozygotes were bred to each other in order to generate HIF-1α null homozygous mice. Null homozygous mice were isolated at mid-gestation and analyzed for gross morphological defects. One obvious difference at this stage (E9.5) is the greatly disturbed vascularization of the embryonic yolk sac. The yolk sacs from mutant embryos exhibit a complete lack of vascular organization when compared with wild-type embryos (Figure 5C). There is no organized branching of the vasculature, although there are fully formed vessels and red blood cells. This demonstrates that HIF-1α is essential for the proper formation of this vascular network, and implies that oxygen levels function as a key determinant of capillary arrangement and organization in this tissue.

Abnormal neural development and cephalic vascularization in HIF-1α mutant mice

HIF-1α null embryos were clearly discernible *in utero* beginning at E8.0, when the null mutant embryos are smaller and have reduced and somewhat convoluted neural folds. E8.0 is also the stage in which we see high expression of the HIF-1α–lacZ knock-in fusion in the cephalic region (Figure 5G).

At E8.5, embryonic expression of the HIF-1α–lacZ fusion in the neural fold is localized to the innermost layer of cells (arrow, Figure 5H). Loss of HIF-1α expression at this stage and in this location is correlated with the aberrantly formed and incompletely closed neural fold seen in null mutants (Figure 5A). In addition, the HIF-1α null mutants have a reduced number of somites (Figure 5A), another site of a distinct pattern of HIF-1α–lacZ expression (Figure 5F). At E9.5, the null mutant embryos (Figure 5B) are much smaller than their wild-type littermates; interestingly, the neural folds at this stage are still not closed, but neural vesicles have begun to form on either side of the head, resulting in paired balloon-like structures in the fore-, mid- and hindbrain regions of the embryo.

Because loss of HIF-1α has a profound effect on VEGF expression and VEGF plays an essential role in embryonic development, we examined the vascularization pattern of HIF-1α null embryos. In embryos stained for the endothelial cell marker CD31 (Figure 5D and E) the requirement for HIF-1α in embryonic vascularization is clear. The neural folds have a very small number of capillaries and no vascular network, and the intersomitic vasculature is interrupted. This result indicates that HIF-1 is an essential regulator of cephalic vascularization. Despite the abnormalities in capillary network formation seen in the null embryos, the dorsal aorta is present but reduced in size, and the heart is almost normally sized and was found beating in both E8.5 and E9.5 embryos (Figure 5A and B).

Increased hypoxia and apoptosis in HIF-1α null embryos

In order to determine whether the loss of HIF-1α had any effect on levels of embryonic oxygenation, we undertook a study of wild-type and null embryos using the nitroimidazole hypoxia marker EF5 (Lee *et al.*, 1996). This small molecule forms adducts to macromolecules in reducing microenvironments and thus can be used to detect hypoxic

regions in tissues (Lord *et al.*, 1993; Lee *et al.*, 1996). This is accomplished through detection of these adducts by EF5-specific monoclonal antibody binding, as shown in Figure 6C. There was a striking increase in the binding of EF5 in the null mutant embryos. This binding was seen in most embryonic structures, but was highest in the neural ectoderm and somites. The increase in binding was quantified by CCD measurement of pixel illumination per embryo section and revealed a 10.5-fold increase in bound antibody in a null embryo versus its wild-type littermate.

We wished to determine whether the increase in embryonic hypoxia was reflected in an increase in apoptotic cell death. To assay this, we measured apoptosis in wild-type and null embryos by TUNEL assay, as shown in Figure 6D. As can be seen, there is a significant increase in apoptotic cell number in the interior of the null mutant

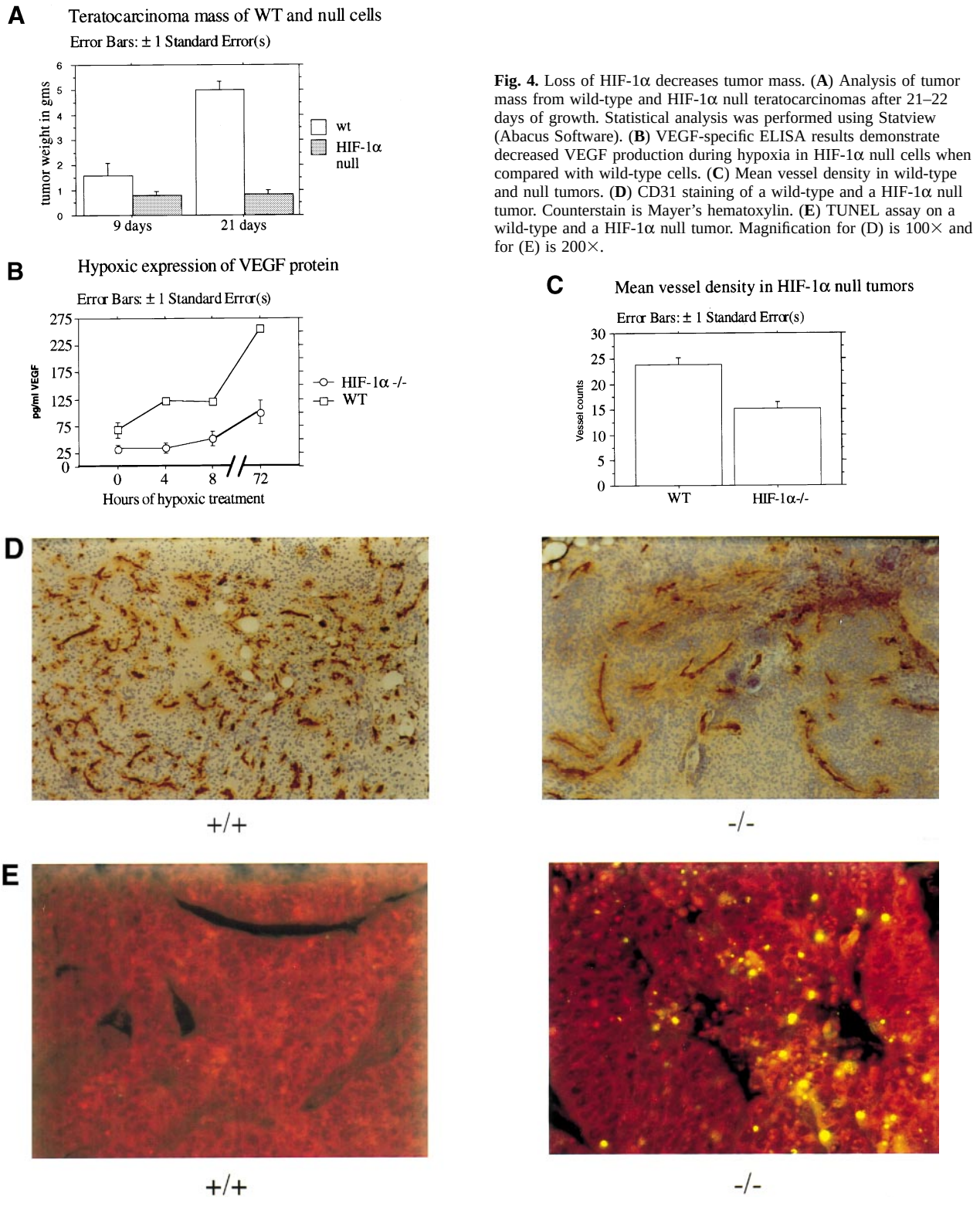

Fig. 4. Loss of HIF-1α decreases tumor mass. (**A**) Analysis of tumor mass from wild-type and HIF-1α null teratocarcinomas after 21–22 days of growth. Statistical analysis was performed using Statview (Abacus Software). (**B**) VEGF-specific ELISA results demonstrate decreased VEGF production during hypoxia in HIF-1α null cells when compared with wild-type cells. (**C**) Mean vessel density in wild-type and null tumors. (**D**) CD31 staining of a wild-type and a HIF-1α null tumor. Counterstain is Mayer's hematoxylin. (**E**) TUNEL assay on a wild-type and a HIF-1α null tumor. Magnification for (D) is 100× and for (E) is 200×.

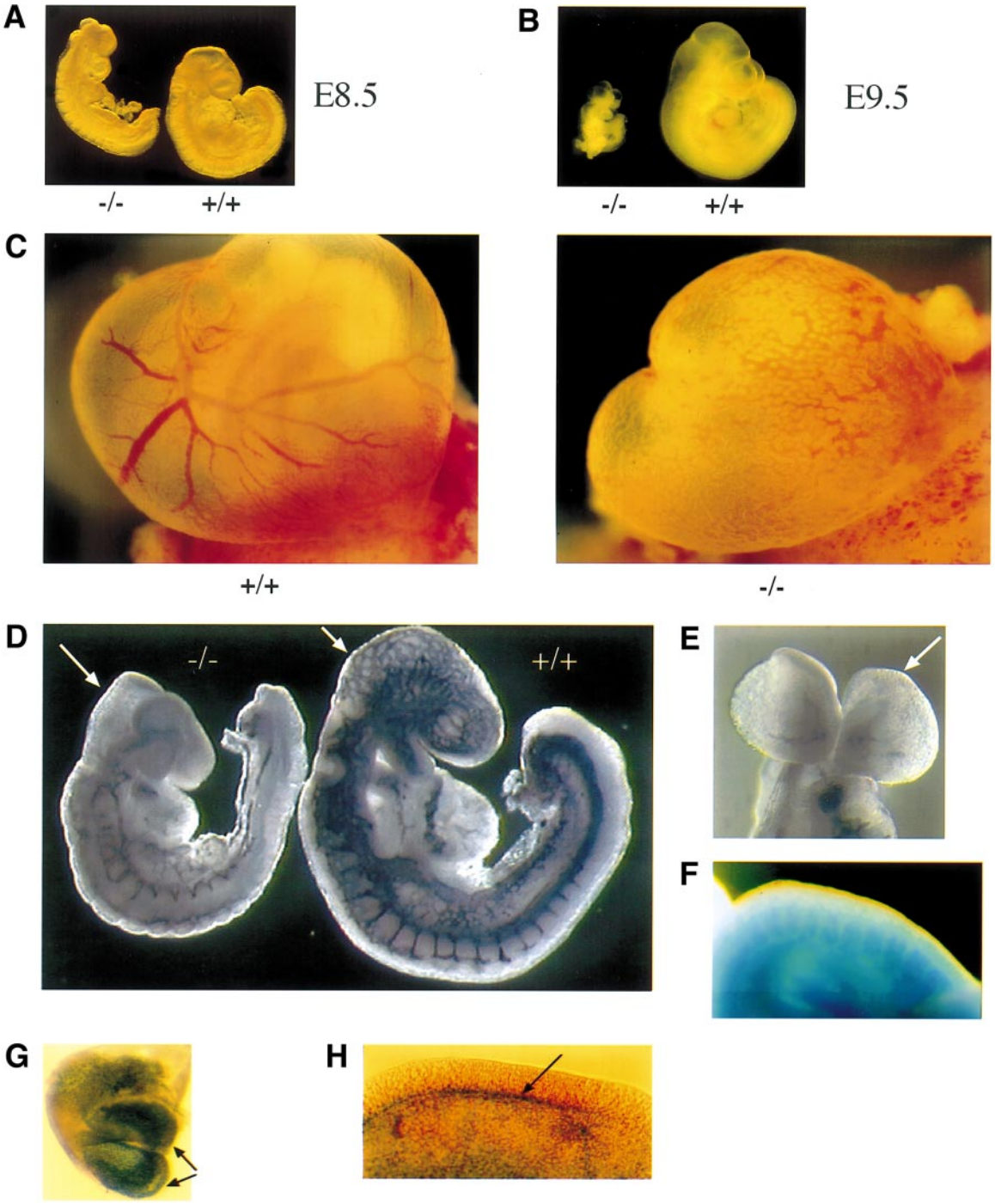

Fig. 5. Gross morphological characterization, whole-mount immunohistochemistry and lacZ staining of HIF-1α null embryos obtained from heterozygous crosses. (**A**) E8.5 littermates, at which point the embryos are approximately the same size. (**B**) E9.5 littermates, displaying a substantial size difference. (**C**) Yolk sacs from E9.5 littermates. The HIF-1α null yolk sac shows disorganized vascularization compared with the wild-type. (**D**) E8.5 littermates stained for the endothelial cell-specific marker CD31 demonstrate absence of neural vascularization (arrows) and incomplete somitic vascularization. (**E**) Closer view of the neural folds of an E8.5 HIF-1α null embryo stained for CD31 (arrow). (**F**, **G** and **H**) Staining of heterozygous embryos carrying an in-frame *lacZ* fusion at the HIF-1α locus. A distinct pattern of somitic expression is seen in (F), an E8.5 embryo. At E8.0 (G) we see intense staining in the neural folds (arrows) while at E8.5 (H) the expression appears to be localized to a layer of cells lining the inner neural ectoderm (arrow).

neural fold, correlated with increased hypoxia in this area and an absence of normal vascularization.

Loss of PGK expression in mutant embryos

The neural fold is clearly the site of significant levels of HIF-1α expression, and we wished to correlate this with expression of HIF-1 target genes. Due to the significant role HIF-1α plays in normoxic and hypoxic PGK expression, as evidenced by the Northern blot data (Figure 2A and C), we chose to examine its regulation in the embryo. *In situ* data (Figure 6A and B) reveal that PGK is also largely HIF-1α dependent in the embryo as loss of HIF-1α completely ablates PGK expression. The expression of PGK is highest in the margins of the neural fold (Figure 6A and B, arrows), implying that glycolytic activity may contribute to the normal development of this tissue, and

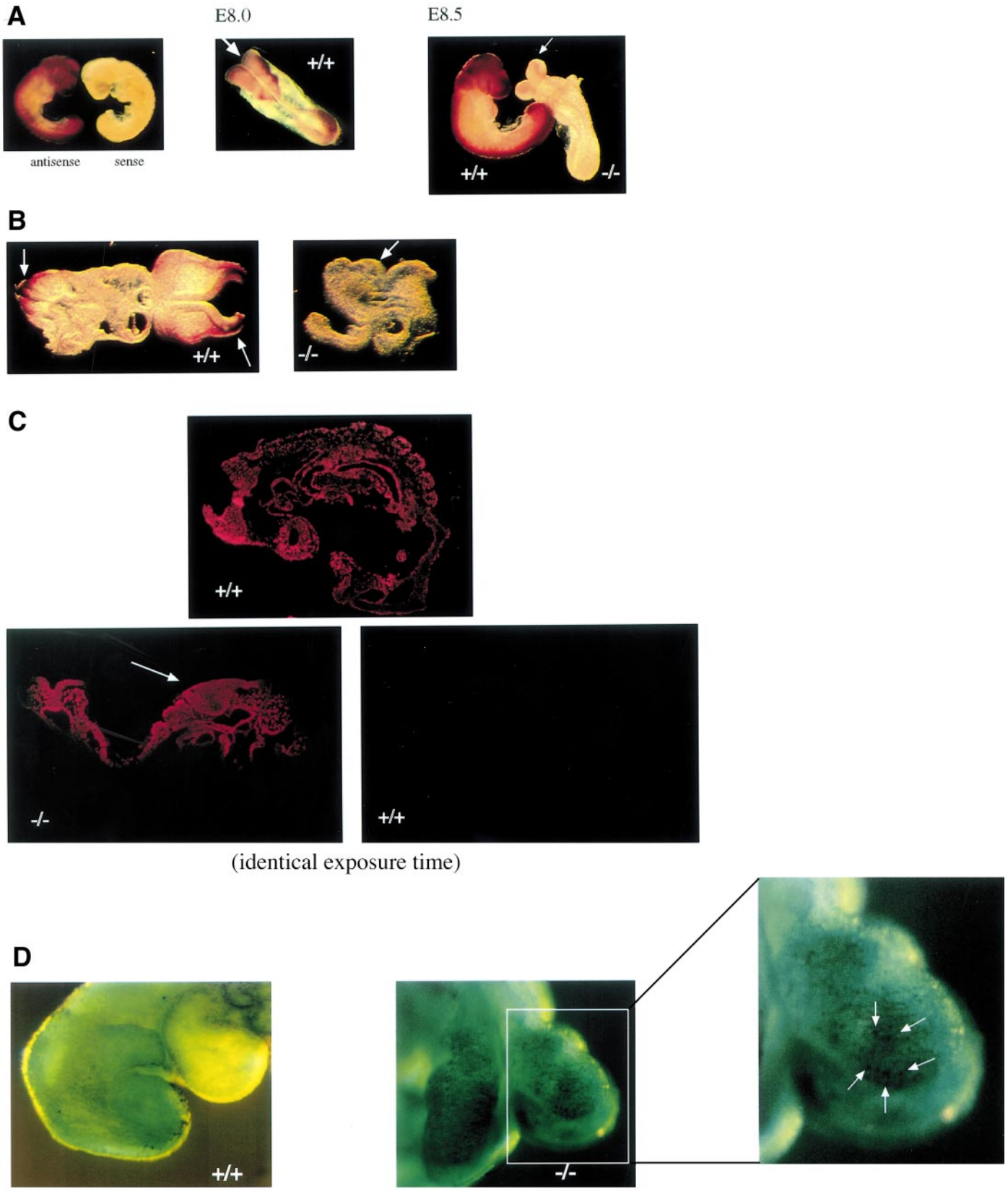

Fig. 6. Analysis of PGK expression in embryos and characterization of hypoxia and apoptosis in E8.5 embryos. (**A**) Whole mount *in situ*s of wild-type and HIF-1α null embryos showing intense expression of PGK in the neural tube region and complete loss of this expression in null embryos (arrows). (**B**) Vibratome sections of a wild-type and null embryo stained for PGK expression, demonstrating the neural-specific pattern of expression (arrows) in the wild-type embryo and lack of such expression in the null embryo (arrow). (**C**) EF5 staining of frozen sections from wild-type and null embryos. When exposure time is held constant for the null and wild-type embryos, it becomes clear that there is a significant difference in the level of hypoxia in the null embryo. (**D**) Whole mount TUNEL assay on wild-type and null embryos. There are a few scattered apoptotic cells in the head of the wild-type embryo while the neural folds of the null embryo are littered with darkly staining apoptotic cells (close up, arrows).

that its absence is contributing to the abnormal neural fold formations seen in HIF-1α null mutants.

Discussion

Hypoxia has been proposed to regulate many physiological and pathological processes. In order to understand better the significance of the hypoxic response in such processes, we have created a null mutation at the HIF-1α locus, generating both null ES cells and null mutant mice. In the null ES cells, we have completely abolished HIF-1 binding to both the EPO HRE and the VEGF HRE, as assayed by electromobility shift assays. This result is interesting in that it indicates that HIF-1α is the primary dimerization partner of ARNT in binding both EPO HRE and VEGF HRE sequences. Also, at least in ES cells, HIF-2α is not involved in binding the VEGF HRE under hypoxia, as has been proposed by others (Ema *et al*., 1997).

Northern blot analysis, quantitation and, in the case of PGK, *in situ* hybridization reveal that HIF-1α is essential for the basal expression of two genes, LDH and PGK, and the hypoxic and hypoglycemic induction of a number of other, more disparate genes. In the case of PGK, LDH and ALDA, the hypoxically induced increase in message is completely abolished in the HIF-1α null cells. The profound effect on these genes indicates that HIF-1α plays a key role in the induction of a glycolytic response in tissues under hypoxic stress.

We also see a decreased hypoxic response of GLUT1 in the null cells. This further indicates the importance of hypoxic transcriptional induction in cellular metabolism. It also underscores the importance of glycolysis during hypoxic stress; curiously, we saw no differential effect between the mutants and wild-type cells during low glucose or hypoxic cell conditions. This may be the result of the somewhat unusual characteristics of ES cell growth, however, and be unrelated to the role of HIF-1α in the adult organism.

VEGF is another HIF-1 target gene that is affected by the loss of HIF-1α. Quantitation of VEGF mRNA indicates that the hypoxic regulation of the gene is severely affected in HIF-1α null cells. This is not surprising given the considerable evidence that VEGF is regulated by hypoxia-induced transcriptional activation, although it has also been shown to be strongly regulated by increased mRNA stability (Finkenzeller *et al*., 1995; Ikeda *et al*., 1995; Levy *et al*., 1995, 1996; Shima *et al*., 1995). It is surprising, given this other important mode of transcript regulation, that we see such a marked decrease in both the mRNA levels and the secreted protein. It is also striking that the kinetics of VEGF expression in response to hypoxia change considerably in the HIF-1α null cells: there is a slight increase in RNA and secreted protein levels at 4 h of hypoxia, and only a very gradual up-regulation of protein expression (and no increase in RNA levels) after extended incubation in a hypoxic environment. This result indicates that the primary means of up-regulating VEGF expression may be via transcriptional induction of expression, and that increased mRNA stability plays a more minor role than has been proposed previously (Ikeda *et al*., 1995; Levy *et al*., 1995, 1996; Shima *et al*., 1995)

Gel shift data indicate that there is no redundancy in HIF-1 components in ES cells, as there is no compensation for the loss of HIF-1α at the level of DNA binding. The HIF-1α homolog HIF-2α is expressed *in vivo* primarily by endothelial cells (Ema *et al*., 1997; Hogenesch *et al*., 1997; Tian *et al*., 1997), and there may be tissue-specific activation of the gene necessary for DNA binding during hypoxia. Thus there may be functional redundancy in some tissue types, although we see no evidence for this at the level of ES cells or embryos. Further analysis of possible tissue-specific redundancy will require the creation of HIF-1α conditional knockouts and analysis of tissues individually targeted for the loss of HIF-1α.

The role of hypoxia in tumors, from inducing angiogenesis to selecting for p53 null cells, has been well studied (Shweiki *et al*., 1992; Potgens *et al*., 1995; Forsythe *et al*., 1996; Damert *et al*., 1997; Gassmann *et al*., 1997). Using the HIF-1α null ES cells as a tool, we were able to characterize the contribution that the transcriptional hypoxic response makes to tumor growth. Teratocarcinomas lacking HIF-1α exhibited a substantial decrease in tumor mass when compared with wild-type teratocarcinomas (Figure 4A). This result indicates that an intact HIF-1 response is essential to sustain rapid growth in the tumor microenvironment.

Our results in cell culture, where no significant difference in hypoxic cell survival between wild-type and null cells was seen, suggests that the role of HIF-1 in expansion of a solid tumor mass is non-cell autonomous. The role of VEGF as a paracrine regulator of angiogenesis makes it a logical candidate effector of the tumor phenotype. Indeed, when VEGF protein levels were assayed under hypoxic conditions, we found a 4-fold mean decrease in secreted protein in the null cells. This striking difference between wild-type and null cells indicates that angiogenic insufficiency may be one cause of the decreased tumor mass. This finding is bolstered further by the decrease in vessel numbers found in the null tumors, clearly tying hypoxic response through HIF-1α to tumor vascularization.

One exciting finding of this work is the demonstration that HIF-1α, and by extension the transcriptional response to hypoxia, plays an essential role in embryonic development and vascularization. Although the targeted mutation of the VEGF locus and its receptors demonstrated that the angiogenic response of this factor was required for embryonic vascularization, little is known about exactly how the developing vasculature and capillary networks are organized. The role of HIF-1α in this process is perhaps most strikingly seen in the capillary network of the embryonic yolk sac. Here, there is no arborization of the vasculature; the vessels in the mutant yolk sac are spread evenly over the entire tissue, and are roughly equidistant. This highly abnormal and very ineffective organization demonstrates that HIF-1α is required not for vessel formation *per se*, but for the organization and centralization of vascular networks. One possible explanation for this may be that the vascularization process is driven by microenvironmental hypoxia, where small regions of low oxygen pressure at the cellular level drive the angiogenic response, in a manner mediated by the HIF-1α transcriptional response.

In the embryo proper, it is clear that there is an even more profound role for HIF-1α in regulating vascularization. Here, we see an almost complete absence of

vascularization in the head, although there is a normally sized heart and dorsal aorta. This may indicate that HIF-1α expression is more critical for driving the formation of capillary networks than for the formation of major vessels, whose morphogenesis is severely affected, by contrast, in the VEGF knockout embryo.

The loss of vascular bed formation in the embryonic cephalus indicated that this was a critical area for HIF-1-mediated transcription. We analyzed this neuroectodermal role using a number of methods. First, staining of the *lacZ* knock-in embryos indicated that the neural fold is an area of abundant and early (E8.0) HIF-1α expression. Second, whole mount *in situ* staining for one of the most highly regulated HIF-1 target genes, PGK, showed that it is almost completely dependent on HIF-1α for embryonic expression. These results may indicate that increased HIF-1α activity leads to the high levels of aerobic glycolysis observed at this stage of embryonic development by many investigators (Akazawa *et al*., 1994; Hunter and Tugman, 1995; Matsumoto *et al*., 1995; Shepard *et al*., 1997). These mutants are thus a model for studying neuroectodermal expression of glycolytic enzymes and activity, which has in turn been linked to such phenomena as defects in neural tube closure in diabetes (Shepard *et al*., 1997). Further study will be required, however, in order to separate this effect of HIF-1 activity from its role in the transcriptional control of angiogenesis.

We have presented evidence for the first time that embryonic hypoxia, as demarcated by the EF5 molecule, is controlled by the HIF-1α transcription factor. This is an exciting finding, and one that demonstrates that HIF-1α is controlling a downstream program of target genes that actually regulate tissue oxygenation. The manifestation of target gene activation probably includes angiogenesis, but could also involve glycolysis as a determinant of cell survival in poorly vascularized tissues, and perhaps other activities that are still unknown. It is clear that HIF-1-mediated regulation of transcription is a very important mechanism for coping with microenvironmental stress. What is also clear from this study is that the stress itself is regulating the process of embryonic organization and growth. In addition, it appears that the culmination of decreased target gene expression, inefficient vascularization and increased hypoxia contributes to a higher degree of neuroectodermal apoptosis in the null embryos. All of these factors clearly point to HIF-1 transcription as a primary determinant of embryonic morphogenesis.

Materials and methods

Construction of the HIF-1α targeting vector

A 345 bp fragment of the mouse HIF-1α cDNA was generated by low stringency PCR on mouse embryonic fibroblast cDNA with primers from the human HIF-1α gene: 5′-GAGAAATGCTTACACACAGAAA-3′ and 5′-CGGTAATTCTTTCATCACAATA-3′ (Wang *et al*., 1995). This fragment was used to obtain three overlapping 129/SvJ BAC clones from Genome Systems, Inc.

A targeting vector was constructed in which the HLH region in exon 2 was replaced by a neomycin resistance cassette. The pMC1neo poly(A) neomycin resistance gene (Stratagene) was cloned into a *Bgl*II site in exon 2 and replaced the HLH region and intron 2 of HIF-1α. A second targeting vector was constructed which contained an in-frame fusion of the *lacZ* gene followed by a *loxP*-flanked *neo*. In this case, the *lacZ* gene was cloned into an *Xba*I site in exon 2, creating an in-frame fusion, and followed by a PCR-generated *loxP*-flanked *neo*. The HLH region and intron 2 were also deleted in this construct. The final constructs contained 0.7 kb of 5′ homology and 7.0 kb of 3′ homology. The constructs were linearized and electroporated into R1 ES cells (Nagy and Rossant, 1992). After selection under 150 μg/ml G418, clones were analyzed by *Bam*HI digest and hybridized to a 5′ external probe. HIF-1α null clones were obtained by high G418 selection, at 3 and 4 mg/ml, as described in Mortensen *et al*. (1992). The *lacZ*-containing clones were transiently transfected with a *cre* recombinase-expressing plasmid and assayed for loss of the neomycin resistance gene by Southern blotting and PCR. Chimeric mice were generated via injection of targeted ES cells into C57Bl/6 blastocysts (Papaioannou and Johnson, 1992).

Electromobility shift assay

Preparation of nuclear extracts and electromobility shift assays were performed as described in Semenza and Wang (1992). Nuclear extracts were isolated from normoxic and hypoxic (5 h hypoxia) cells by incubation of the cells in buffer A [10 mM Tris–HCl (pH 7.8), 1.5 mM $MgCl_2$, 10 mM KCl] followed by 10 strokes with a Dounce homogenizer, type-B pestle. After isolation of nuclei, they were lysed by incubation with buffer C [0.42M KCl, 20 mM Tris–HCl (pH 7.8), 1.5 mM $MgCl_2$, 20% glycerol] and the nuclear extract underwent a final dialysis against buffer D [20 mM Tris–HCl (pH 7.8), 0.1 M KCl, 0.2 mM EDTA, 20% glycerol]. Both buffer A and buffer C were supplemented with 0.5 mM dithiothreitol (DTT), 0.4 mM phenylmethylsulfonyl fluoride, 2 μg/ml leupeptin, 2 μg/ml pepstatin, 2 μg/ml aprotinin and 1 mM sodium orthovanadate. Protein concentration was determined using a Bio-Rad assay.

Binding conditions were 5 μg protein, 10 mM Tris–HCl (pH 7.8), 50 mM KCl, 50 mM NaCl, 1 mM $MgCl_2$, 1 mM EDTA, 5 mM DTT, 5% glycerol, 0.1 μg of denatured calf thymus DNA, 1 ng of ^{32}P end-labeled oligonucleotide probe and a 25 min incubation at room temperature. The binding sites used correspond to the 18 bp HRE from the EPO gene (Semenza and Wang, 1992) and the 24 bp HRE from the VEGF gene (Forsythe *et al*., 1996). Samples were run out on a 6% acrylamide/0.25× TBE gel at 22 mA for 5 h at 4°C.

Northern blot analysis

ES cells were grown in Dulbecco's modified Eagle's medium (DMEM) supplemented with 16% fetal calf serum (FCS) and leukemia inhibitory factor (LIF). Cells cultured for the indicated times were washed once with phosphate-buffered saline (PBS) and RNA was extracted with TRIzol reagent (Gibco-BRL) according to the manufacturer's protocol. Thirty μg of total RNA was loaded per lane, run on a 1% denaturing agarose gel and hybridized with cDNA probes. Probes for the following genes were generated via RT–PCR: PGK, ALDA, LDH, pyruvate kinase M (PK), GLUT1, VEGF and HIF-2α. The ARNT probe was purchased from Genome Systems. Equal loading was monitored by ethidium bromide staining of 28S rRNA.

Dot–blot analysis was performed with a MilliBlot (Millipore) vacuum apparatus. Ten μg of total RNA was loaded per dot and hybridized with cDNA probes. Quantitation was performed with a General Dynamics phosphorimager, model 445SI and ImageQuaNT software (General Dynamics).

Cell viability assay

For the hypoxia experiment, cells were grown at 1% O_2 in DMEM supplemented with 16% FCS and LIF. For the low glucose experiment, cells were grown in glucose-free DMEM supplemented with 16% FCS and LIF. At each time point, cells were washed once with PBS ($-Mg^{2+}$, $-Ca^{2+}$), trypsinized, stained with trypan blue, and viable cells were counted. Two HIF-1α null cell lines and the R1 cell line (wild-type) were analyzed in triplicate at each time point.

Generation of teratocarcinomas

A total of 5×10^6 ES cells in 100 μl of PBS were injected subcutaneously intra-scapularly into immunocompromised mice [5- to 8-week-old RAG-1 –/– males in a FVB/N background (Mombaerts *et al*., 1992)]. Data were obtained from 11 wild-type and nine HIF-1α null tumors, 21 days post-injection.

VEGF ELISA

VEGF quantitation was performed using the Quantikine M Mouse VEGF Immunoassay kit (R&D Systems) according to the manufacturer's protocol. Conditioned medium was incubated with a mouse-specific VEGF polyclonal antibody bound to a microtiter plate. After several washes, a second incubation was performed with an enzyme-linked mouse-specific VEGF polyclonal antibody. Samples consisted of condi-

tioned ES cell media from wild-type and null cells exposed to hypoxia for the indicated time.

Tumor histology

Sections were cut from fresh frozen tumors and stained for CD31. Slides were treated with acetone, rinsed with PBS and blocked with 5% rabbit serum in PBS for 30 min. The sections underwent a 1 h incubation with a 1:100 dilution of the anti-CD31 antibody, MEC13.3 (Pharmingen), followed by a 30 min incubation with a biotinylated rabbit anti-rat secondary antibody (Vector Laboratories, Inc.) diluted 1:400. An avidin-biotinylated horseradish peroxidase (HRP) complex (Vectastain Elite ABC kit) was used to detect the antibody and color was developed with a DAB kit (both from Vector Laboratories, Inc.). Sections were counterstained with Mayer's hematoxylin and mounted. Blood vessel counts were carried out from random fields chosen blindly and counted for CD31 staining.

Formalin-fixed, paraffin-embedded sections from teratocarcinomas were analyzed for apoptosis via TUNEL assay. Staining was performed with the Apoptosis Detection System, Fluorescein (Promega) as described in the manufacturer's protocol.

Whole mount CD31 and lacZ staining

CD31 staining was carried out as described in Schlaeger *et al*. (1995). Embryos were dissected out of the yolk sac in PBS with 0.1% bovine serum albumin (BSA) and fixed overnight in 4% paraformaldehyde at 4°C. The following day, the embryos were dehydrated and endogenous peroxidase activity was blocked by an incubation in 5% H_2O_2 in MeOH. After blocking in PBSMT (3% instant skim milk, 0.1% Triton X-100, PBS) they were then incubated overnight at 4°C with the anti-CD31 antibody MEC13.3 (Pharmingen) diluted 1:50 in PBSMT. The following day, the embryos underwent five 1 h washes in PBSMT, and then were incubated overnight at 4°C with an HRP-conjugated secondary antibody (Pharmingen), diluted 1:200 in PBSMT. After post-secondary washes in PBSMT, color was developed using a DAB kit (Vector Laboratories, Inc.) with 0.3 mg/ml DAB, 0.5% $NiCl_2$ and 0.03% H_2O_2.

For the lacZ staining, embryos were generated via tetraploid fusion (Nagy and Rossant, 1992) and stained as described in Bonnerot and Nicolas (1993). Embryos were dissected out of the yolk sac in PBS and fixed for 20 min in 4% paraformaldehyde at 4°C. The embryos were then permeabilized in 0.01% deoxycholate, 0.02% NP-40 in PBS for 10 min at room temperature and stained in a histochemical reaction mixture (1 mg/ml X-gal, 4 mM potassium ferricyanide, 4 mM potassium ferrocyanide, 2 mM $MgCl_2$) overnight at 30°C.

Apoptosis, EF5 and PGK staining of embryos

Whole-mount apoptosis staining was performed on E8.5 embryos with the TACS *In Situ* Apoptosis Detection kit (Trevigen, Inc.). Embryos were dissected out in PBS and fixed in 4% paraformaldehyde overnight at 4°C, followed by MeOH dehydration. Upon rehydration, embryos were stained according to the manufacturer's protocol with the following modifications. Embryos were permeabilized with Cytopore IHC (Trevigen, Inc.) for 1 h at room temperature. Endogenous peroxidase activity was removed with a 5 min incubation in 3% H_2O_2 in MeOH. Embryos were counterstained with a 0.05% methyl green solution.

EF5 staining (Lord *et al*., 1993) was performed on fixed frozen sections from E8.5 embryos. Pregnant heterozygous females were injected with 10 mM EF5 at 1% of body weight. Three hours later, the embryos were dissected out in cold PBS and fixed in 4% paraformaldehyde for 2 h. Embryos were incubated overnight in 30% sucrose, embedded in OCT and 10 μm thick sections were cut. For staining, the slides were dipped in acetone for 10 min at 4°C, air dried and rinsed in PBS. Blocking was performed with 5% mouse serum in PBS for 30 min at room temperature. Sections were stained with a mouse anti-EF5 Cy3-conjugated antibody, diluted 1:25 in 3% BSA and PBS, for 2 h at room temperature. Slides were rinsed with PBS for 5 min and mounted with an aqueous mounting medium. Quantitation of EF5 binding was done using the Leica DMLD phototube CCD to measure light levels from the fluorescent samples at whole section (×25) magnification.

Whole-mount *in situ* hybdridizations were performed using a digoxigenin-labeled riboprobe generated from a 485 bp PGK cDNA fragment cloned into the pGEM-T Easy Vector (Promega). The embryos were dissected out in PBS, fixed for 2 h in 4% paraformaldehyde and stored in 70% EtOH prior to staining. Upon rehydration, embryos were treated with 10 μg/ml proteinase K, washed in 2 mg/ml glycine and refixed with 0.2% glutaraldehyde in 4% paraformaldehyde. Embryos went through a pre-hybridization incubation at 70°C followed by an overnight hybridization at 70°C with the digoxigenin-labeled PGK probe at 1 μg/ml. Embryos were washed twice in solution 1 (50% formamide, 5× SSC, 1% SDS) and twice in solution 2 (50% formamide, 2× SSC), all for 30 min at 70°C. Embryos were blocked with heat-treated 10% goat serum and incubated overnight at 4°C with anti-digoxigenin antibody. Following several washes in TBST [140 mM NaCl, 2.6 mM KCl, 25 mM Tris–HCl (pH 7.5), 0.1% Tween-20] and NTMT [100 mM NaCl, 100 mM Tris–HCl (pH 9.5), 50 mM $MgCl_2$, 0.1% Tween-20], color was developed in NTMT with 4.5 μl/ml NBT and 3.5 μl/ml BCIP. Both TBST and NTMT were supplemented with 2 mM levamisole. Sections were cut with a vibratome and mounted for photography.

Acknowledgements

We thank Drs Cameron Koch and Edith Lord for the kind gift of EF5 and anti-EF5 antibody, and Jeremy Grunstein and Marian Dealy for work done in the early stages of the project. R.S.J. wishes to acknowledge helpful comments and advice from Drs Peter Carmeliet, Amato Giaccia, Robert Warren, Michael David and Robert Rickert. We would also like to acknowledge excellent technical assistance from Rennie Wolfe and the Transgenic Analysis Core of the Medical College of Georgia. This work was supported by start-up funds from the Department of Biology, UCSD.

References

Akazawa,S., Unterman,T. and Metzger,B.E. (1994) Glucose metabolism in separated embryos and investing membranes during organogenesis in the rat. *Metabolism*, **43**, 830–835.

Banai,S., Shweiki,D., Pinson,A., Chandra,M., Lazarovici,G. and Keshet,E. (1994) Upregulation of vascular endothelial growth factor expression induced by myocardial ischaemia: implications for coronary angiogenesis. *Cardiovasc. Res*., **28**, 1176–1179.

Blanchard,K.L., Fandrey,J., Goldberg,M.A. and Bunn,H.F. (1993) Regulation of the erythropoietin gene. *Stem Cells*, **11** Suppl. 1, 1–7.

Bonnerot,C. and Nicolas,J.-F. (1993) Application of *LacZ* gene fusions to post-implantation development. In Wasserman,P. and DePamphilis,M.L. (eds), *Guide to Techniques in Mouse Development*. Academic Press, New York, pp. 451–469.

Brown,J.M. and Giaccia,A.J. (1994) Tumour hypoxia: the picture has changed in the 1990s. *Int. J. Radiat. Biol*., **65**, 95–102.

Bunn,H.F. and Poyton,R.O. (1996) Oxygen sensing and molecular adaptation to hypoxia. *Physiol. Rev.*, **76**, 839–885.

Carmeliet,P. *et al*. (1996) Abnormal blood vessel development and lethality in embryos lacking a single VEGF allele. *Nature*, **380**, 435–439.

Dachs,G.U., Patterson,A.V., Firth,J.D., Ratcliffe,P.J., Townsend,K.M., Stratford,I.J. and Harris,A.L. (1997) Targeting gene expression to hypoxic tumor cells. *Nature Med*., **3**, 515–520.

Damert,A., Machein,M., Breier,G., Fujita,M.Q., Hanahan,D., Risau,W. and Plate,K.H. (1997) Up-regulation of vascular endothelial growth factor expression in a rat glioma is conferred by two distinct hypoxia-driven mechanisms. *Cancer Res*., **57**, 3860–3864.

Ema,M., Taya,S., Yokotani,N., Sogawa,K., Matsuda,Y. and Fujii-Kuriyama,Y. (1997) A novel bHLH-PAS factor with close sequence similarity to hypoxia-inducible factor 1 alpha regulates the VEGF expression and is potentially involved in lung and vascular development. *Proc. Natl Acad. Sci. USA*, **94**, 4273–4278.

Fernandez-Salguero,P. *et al*. (1995) Immune system impairment and hepatic fibrosis in mice lacking the dioxin-binding Ah receptor. *Science*, **268**, 722–726.

Ferrara,N., Carver-Moore,K., Chen,H., Dowd,M., Lu,L., O'Shea,K.S., Powell-Braxton,L., Hillan,K.J. and Moore,M.W. (1996) Heterozygous embryonic lethality induced by targeted inactivation of the VEGF gene. *Nature*, **380**, 439–442.

Finkenzeller,G., Technau,A. and Marme,D. (1995) Hypoxia-induced transcription of the vascular endothelial growth factor gene is independent of functional AP-1 transcription factor. *Biochem. Biophys. Res. Commun*., **208**, 432–439.

Forsythe,J.A., Jiang,B.H., Iyer,N.V., Agani,F., Leung, S.W., Koos,R.D. and Semenza,G.L. (1996) Activation of vascular endothelial growth factor gene transcription by hypoxia-inducible factor 1. *Mol. Cell. Biol*., **16**, 4604–4613.

Gassmann,M., Kvietikova,I., Rolfs,A. and Wenger,R.H. (1997) Oxygen- and dioxin-regulated gene expression in mouse hepatoma cells. *Kidney Int*., **51**, 567–574.

Graeber,T.G., Osmanian,C., Jacks,T., Housman,D.E., Koch,C.J., Lowe,S.W. and Giaccia,A.J. (1996) Hypoxia-mediated selection of cells with diminished apoptotic potential in solid tumours. *Nature*, **379**, 88–91.

Hirose,K. *et al*. (1996) cDNA cloning and tissue-specific expression of a novel basic helix–loop–helix/PAS factor (Arnt2) with close sequence similarity to the aryl hydrocarbon receptor nuclear translocator (Arnt). *Mol. Cell. Biol*., **16**, 1706–1713.

Hogenesch,J.B., Chan,W.K., Jackiw,V.H., Brown,R.C., Gu,Y.Z., Pray-Grant,M., Perdew,G.H. and Bradfield,C.A. (1997) Characterization of a subset of the basic-helix–loop–helix-PAS superfamily that interacts with components of the dioxin signaling pathway. *J. Biol. Chem*., **272**, 8581–8593.

Hunter,E.S.R. and Tugman,J.A. (1995) Inhibitors of glycolytic metabolism affect neurulation-staged mouse conceptuses *in vitro*. *Teratology*, **52**, 317–323.

Ikeda,E., Achen,M.G., Breier,G. and Risau,W. (1995) Hypoxia-induced transcriptional activation and increased mRNA stability of vascular endothelial growth factor in C6 glioma cells. *J. Biol. Chem*., **270**, 19761–19766.

Ladoux,A. and Frelin,C. (1993) Hypoxia is a strong inducer of vascular endothelial growth factor mRNA expression in the heart. *Biochem. Biophys. Res. Commun*., **195**, 1005–1010.

Lee,J., Siemann,D.W., Koch,C.J. and Lord,E.M. (1996) Direct relationship between radiobiological hypoxia in tumors and monoclonal antibody detection of EF5 cellular adducts. *Int. J. Cancer*, **67**, 372–378.

Levy,A.P., Levy,N.S., Wegner,S. and Goldberg,M.A. (1995) Transcriptional regulation of the rat vascular endothelial growth factor gene by hypoxia. *J. Biol. Chem*., **270**, 13333–13340.

Levy,A.P., Levy,N.S. and Goldberg,M.A. (1996) Post-transcriptional regulation of vascular endothelial growth factor by hypoxia. *J. Biol. Chem*., **271**, 2746–2753.

Liu,Y., Cox,S.R., Morita,T. and Kourembanas,S. (1995) Hypoxia regulates vascular endothelial growth factor gene expression in endothelial cells. Identification of a 5′ enhancer. *Circ. Res*., **77**, 638–643.

Lord,E.M., Harwell,L. and Koch,C.J. (1993) Detection of hypoxic cells by monoclonal antibody recognizing 2-nitroimidazole adducts. *Cancer Res*., **53**, 5721–5726.

Maltepe,E., Schmidt,J.V., Baunoch,D., Bradfield,C.A. and Simon,M.C. (1997) Abnormal angiogenesis and responses to glucose and oxygen deprivation in mice lacking the protein ARNT. *Nature*, **386**, 403–407.

Matsumoto,K., Akazawa,S., Ishibashi,M., Trocino,R.A., Matsuo,H., Yamasaki,H., Yamaguchi,Y., Nagamatsu,S. and Nagataki,S. (1995) Abundant expression of GLUT1 and GLUT3 in rat embryo during the early organogenesis period. *Biochem. Biophys. Res. Commun*., **209**, 95–102.

Mombaerts,P., Iacomini,J., Johnson,R.S., Herrup,K., Tonegawa,S. and Papaioannou,V.E. (1992) RAG-1-deficient mice have no mature B and T lymphocytes. *Cell*, **68**, 869–877.

Mortensen,R.M., Conner,D.A., Chao,S., Geisterfer-Lowrance,A.A. and Seidman,J.G. (1992) Production of homozygous mutant ES cells with a single targeting construct. *Mol. Cell. Biol*., **12**, 2391–2395.

Nagy, A. and Rossant, J. (1992) Production of completely ES-cell derived fetuses. In Joyner,A. (ed.), *Gene Targeting: A Practical Approach*. IRL Press at Oxford University Press, Oxford, UK.

Papaioannou,V.E. and Johnson,R.S. (1992) Production of chimeras and genetically defined offspring from targeted ES cells. In Joyner,A. (ed.), *Gene Targeting: A Practical Approach*. IRL Press at Oxford University Press, Oxford, UK.

Pe'er,J., Shweiki,D., Itin,A., Hemo,I., Gnessin,H. and Keshet,E. (1995) Hypoxia-induced expression of vascular endothelial growth factor by retinal cells is a common factor in neovascularizing ocular diseases. *Lab. Invest*., **72**, 638–645.

Potgens,A.J., Lubsen,N.H., van Altena,M.C., Schoenmakers,J.G., Ruiter,D.J. and de Waal,R.M. (1995) Vascular permeability factor expression influences tumor angiogenesis in human melanoma lines xenografted to nude mice. *Am. J. Pathol*., **146**, 197–209.

Rowlands,J.C. and Gustafsson,J.A. (1997) Aryl hydrocarbon receptor-mediated signal transduction. *Crit. Rev. Toxicol*., **27**, 109–134.

Schlaeger,T.M., Qin,Y., Fujiwara,Y., Magram,J. and Sato,T.N. (1995) Vascular endothelial cell lineage-specific promoter in transgenic mice. *Development*, **121**, 1089–1098.

Schmidt,J.V., Su,G.H., Reddy,J.K., Simon,M.C. and Bradfield,C.A. (1996) Characterization of a murine Ahr null allele: involvement of the Ah receptor in hepatic growth and development. *Proc. Natl Acad. Sci. USA*, **93**, 6731–6736.

Semenza,G.L. and Wang,G.L. (1992) A nuclear factor induced by hypoxia via *de novo* protein synthesis binds to the human erythropoietin gene enhancer at a site required for transcriptional activation. *Mol. Cell. Biol*., **12**, 5447–5454.

Semenza,G.L., Nejfelt,M.K., Chi,S.M. and Antonarakis,S.E. (1991) Hypoxia-inducible nuclear factors bind to an enhancer element located 3′ to the human erythropoietin gene. *Proc. Natl Acad. Sci. USA*, **88**, 5680–5684.

Semenza,G.L., Roth,P.H., Fang,H.M. and Wang,G.L. (1994) Transcriptional regulation of genes encoding glycolytic enzymes by hypoxia-inducible factor 1. *J. Biol. Chem*., **269**, 23757–23763.

Shepard,T.H., Tanimura,T. and Park,H.W. (1997) Glucose absorption and utilization by rat embryos. *Int. J. Dev. Biol*., **41**, 307–314.

Shima,D.T., Deutsch,U. and D'Amore,P.A. (1995) Hypoxic induction of vascular endothelial growth factor (VEGF) in human epithelial cells is mediated by increases in mRNA stability. *FEBS Lett*., **370**, 203–208.

Shweiki,D., Itin,A., Soffer,D. and Keshet,E. (1992) Vascular endothelial growth factor induced by hypoxia may mediate hypoxia-initiated angiogenesis. *Nature*, **359**, 843–845.

Stone,J., Itin,A., Alon,T., Pe'er,J., Gnessin,H., Chan-Ling,T. and Keshet,E. (1995) Development of retinal vasculature is mediated by hypoxia-induced vascular endothelial growth factor (VEGF) expression by neuroglia. *J. Neurosci*., **15**, 4738–4747.

Swanson,H.I. and Bradfield,C.A. (1993) The AH-receptor: genetics, structure and function. *Pharmacogenetics*, **3**, 213–230.

Tian,H., McKnight,S.L. and Russell,D.W. (1997) Endothelial PAS domain protein 1 (EPAS1), a transcription factor selectively expressed in endothelial cells. *Genes Dev.*, **11**, 72–82.

Wang,G.L. and Semenza,G.L. (1993a) Characterization of hypoxia-inducible factor 1 and regulation of DNA binding activity by hypoxia. *J. Biol. Chem*., **268**, 21513–21518.

Wang,G.L. and Semenza,G.L. (1993b) General involvement of hypoxia-inducible factor 1 in transcriptional response to hypoxia. *Proc. Natl Acad. Sci. USA*, **90**, 4304–4308.

Wang,G.L. and Semenza,G.L. (1995) Purification and characterization of hypoxia-inducible factor 1. *J. Biol. Chem*., **270**, 1230–1237.

Wang,G.L., Jiang,B.H., Rue,E.A. and Semenza,G.L. (1995) Hypoxia-inducible factor 1 is a basic-helix–loop–helix-PAS heterodimer regulated by cellular O_2 tension. *Proc. Natl Acad. Sci. USA*, **92**, 5510–5514.

Received January 16, 1998; revised March 16, 1998; accepted March 31, 1998

Note added in proof

Iyer *et al*. (1998) have recently published results on a targeted disruption of HIF-1α and see a similar phenotype in the mice to the one we see [*Genes Dev.* (1998), **12**, 149–162].